

# Cancer Cell Invasion

Case Study in Mathematical Modelling

Candidate Number: 1060612

# 1 Introduction

In this paper, we discuss how we can model tumour spreading in a healthy cell population. The invading tumour can be modelled using a nonlinear reaction-diffusion equation, which can be viewed as an extension of the Fisher Equation with Lotka-Volterra competition terms. In the first few sections, we discuss the basics of these models and demonstrate mathematical techniques to analyse them. This is then used to confirm biologically proven results from Gatenby and Gawlinski [1]. Also, we add a wound-healing effect which Gatenby and Gawlinski have been criticised for omitting.

Furthermore, we add treatments to our model and observe how different treatments can reduce the wave speed of the tumour invasion. We believe to the best of our knowledge the addition of treatments to this model has not been done before.

$N \geq 0$	Population density
$L > 0$	Excess concentration of $H^+$ ions
$D > 0$	Diffusion coefficient
$K > 0$	Population carrying capacity
$\alpha > 0$	Competition strength
$r > 0$	Population growth rate
$d_{1,2} > 0$	Death rate of tissue due to $H^+$ ions
$d_3 > 0$	Re-absorption rate of $H^+$ ions

Table 1: Variables in Gatenby and Gawlinski's model

In this paper, we use the variables in Table 1 in our equations.

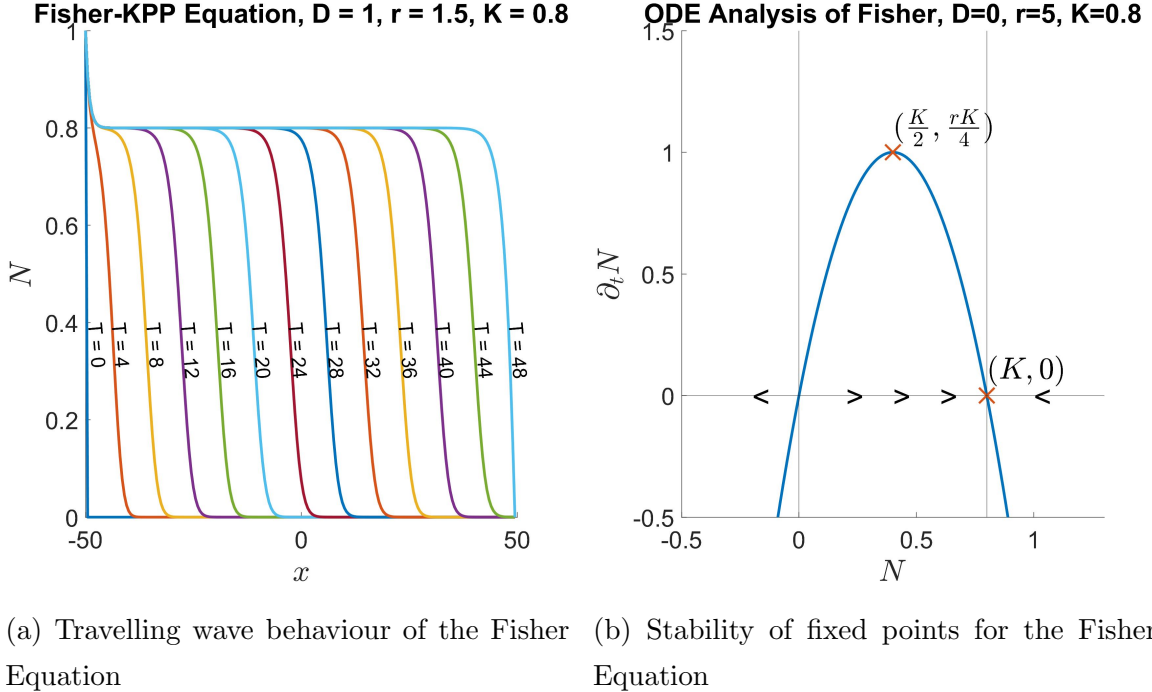
# 2 Fisher's Equation

Firstly, we introduce Fisher's Equation which is a reaction-diffusion equation and models the population dynamics of a system. Fisher's Equation is stated in [2] and it is

$$\partial_t N = D \nabla \cdot \nabla N + rN\left(1 - \frac{N}{K}\right). \quad (1)$$

We would like to know the stability of this system (what the system will become once the wave has passed), we do this by removing the diffusion term i.e.  $D = 0$ .

When  $D = 0$  we get fixed points at  $N = 0$  and  $N = K$ . We can clearly see from the Figure 1b that  $N = 0$  is unstable and  $N = K$  is stable. Therefore, we have taken



(a) Travelling wave behaviour of the Fisher Equation (b) Stability of fixed points for the Fisher Equation

Figure 1: Numerical simulation of Fisher's Equation (1)

each  $x$  position as an individual ODE and when diffusion occurs it slightly displaces the  $N$  off the unstable fixed point  $N = 0$  thus causing it to travel to the stable fixed point  $N = 1$ . This forms the wave shown in Figure 1a. This is an example of diffusion causing instability in a reaction-diffusion equation.

Also, an alternative technique to calculate the stability of the equations is to transform the system into travelling wave coordinates by using  $z = x - ct$ . In this paper, we use the technique of removing diffusion to calculate the stability of more complex partial differential equations.

### 3 Squirrel Model

We now look at a PDE to model the population dynamics of a system. In particular, we will consider the case when grey squirrels were introduced into the UK and model the spread of grey squirrels and how this caused a decline in the red squirrel population.

Therefore, we add an extra species and a Lotka-Volterra competition term to Fisher's Equation. This results in

$$\begin{cases} \partial_t N_G = D_G \nabla^2 N_G + r_G \left(1 - \frac{N_G}{K_G} - \alpha_G N_R\right) N_G, \\ \partial_t N_R = D_R \nabla^2 N_R + r_R \left(1 - \frac{N_R}{K_R} - \alpha_R N_G\right) N_R, \end{cases} \quad (2)$$

where  $\cdot_G, \cdot_R$  represent grey and red squirrels respectively. The PDE (2) is stated in [3]. We are only interested in the domain  $N_G, N_R \geq 0$ . We now non-dimensionalize the system (2) with scalings

$$N_G = \tilde{N}_G K_G, \quad N_R = \tilde{N}_R K_R, \quad t = \frac{\tilde{t}}{r_G}, \quad \vec{x} = \sqrt{\frac{D_G}{r_G}} \tilde{\vec{x}}, \quad (3)$$

where  $\tilde{\cdot}$  represents the scaled variable. We will now define constants

$$r = \frac{r_R}{r_G}, \quad \beta_G = \alpha_G K_R, \quad \beta_R = \alpha_R K_G, \quad D = \frac{D_R}{D_G}, \quad (4)$$

this leads to the PDE system

$$\begin{cases} \partial_{\tilde{t}} \tilde{N}_G = \tilde{\nabla}^2 \tilde{N}_G + \tilde{N}_G \left(1 - \tilde{N}_G - \beta_G \tilde{N}_R\right), \\ \partial_{\tilde{t}} \tilde{N}_R = D \tilde{\nabla}^2 \tilde{N}_R + r \tilde{N}_R \left(1 - \tilde{N}_R - \beta_R \tilde{N}_G\right). \end{cases} \quad (5)$$

### 3.1 Analysis of ODE System

We now remove diffusion from the non-dimensional PDE (5). This leads to the ODE system

$$\begin{cases} \frac{d\tilde{N}_G}{d\tilde{t}} = \tilde{N}_G \left(1 - \tilde{N}_G - \beta_G \tilde{N}_R\right), \\ \frac{d\tilde{N}_R}{d\tilde{t}} = \tilde{N}_R \left(1 - \tilde{N}_R - \beta_R \tilde{N}_G\right) r. \end{cases} \quad (6)$$

We will linearise the system (6) to get the Jacobian matrix which is

$$\begin{bmatrix} \partial_{\tilde{N}_G} \left( \frac{d\tilde{N}_G}{d\tilde{t}} \right) & \partial_{\tilde{N}_R} \left( \frac{d\tilde{N}_G}{d\tilde{t}} \right) \\ \partial_{\tilde{N}_G} \left( \frac{d\tilde{N}_R}{d\tilde{t}} \right) & \partial_{\tilde{N}_R} \left( \frac{d\tilde{N}_R}{d\tilde{t}} \right) \end{bmatrix} = \begin{bmatrix} 1 - 2\tilde{N}_G - \beta_G \tilde{N}_R & -\beta_G \tilde{N}_G \\ -r\beta_R \tilde{N}_R & r \left(1 - 2\tilde{N}_R - \beta_R \tilde{N}_G\right) \end{bmatrix}. \quad (7)$$

We now analyse the stability of the fixed points.

**Extinction**,  $\tilde{N}_G = 0, \tilde{N}_R = 0$ . This fixed point leads to the Jacobian matrix (7) having eigenvalues  $\lambda = 1, \lambda = r$ . Since these eigenvalues are positive the fixed point is unstable.

**Red Squirrel Dominance**,  $\tilde{N}_G = 0, \tilde{N}_R = 1$ . This fixed point leads to the Jacobian matrix (7) having eigenvalues  $\lambda = -r, \lambda = 1 - \beta_G$ . This implies the point is stable for  $\beta_G > 1$  and unstable for  $\beta_G < 1$ . Since grey squirrels outperformed red squirrels in the UK we will take this node to be unstable therefore we must have  $\alpha_G < \frac{1}{K_R}$ .

**Grey Squirrel Dominance,  $\tilde{N}_G = 1, \tilde{N}_R = 0$ .** We find the eigenvalues are  $\lambda = -1, \lambda = r(1 - \beta_R)$ . This implies the point is stable for  $\beta_R > 1$  and unstable for  $\beta_R < 1$ .

**Coexistence,  $\tilde{N}_G = \frac{1-\beta_G}{1-\beta_G\beta_R}, \tilde{N}_R = \frac{1-\beta_R}{1-\beta_G\beta_R}$ .** We are interested in a coexistence state in the region  $\tilde{N}_G, \tilde{N}_R > 0$ . And we want the steady state of red squirrel dominance to be unstable to represent squirrel dynamics in the UK so we have  $1 - \beta_G > 0$  thus we must have  $1 - \beta_G\beta_R > 0$  for  $\frac{1-\beta_G}{1-\beta_G\beta_R} > 0$ . This then implies  $1 > \beta_R$  meaning grey squirrel dominance is unstable. Now we will show for this case the fixed point is stable. We substitute the fixed point into the Jacobian (7) matrix to get

$$\frac{1}{\beta_G\beta_R - 1} \begin{bmatrix} 1 - \beta_G & \beta_G(1 - \beta_G) \\ r\beta_R(1 - \beta_R) & r(\beta_R - 1) \end{bmatrix}. \quad (8)$$

We have the determinant of matrix (8) is  $\frac{r(\beta_G-1)(\beta_R-1)}{1-\beta_G\beta_R} > 0$ . Since all entries to the matrix are negative and the determinant is positive this implies all eigenvalues must be negative. This implies the fixed point is stable.

### 3.2 Simulation of Squirrel Coexistence in 1D

We will solve the PDE system (2) in one spatial dimension. We will use variables  $D_G = 8, D_R = 4, K_R = 1, K_G = 0.8, r_G = r_R = 1, \alpha_R = 1.2$  and  $\alpha_G = 0.8$ . This leads us to our non-dimensional constants from (4) being

$$r = 1, \beta_G = 0.8, \beta_R = 0.96, D = 0.5. \quad (9)$$

We first analyse the PDE when there is no diffusion. So if we follow section 3.1 we get there is a stable coexistence state at  $N_G = K_G\tilde{N}_G \approx 0.6897$  and  $N_R = K_R\tilde{N}_R \approx 0.1724$ . Which has a domain of attraction  $N_G > 0$  and  $N_R > 0$ . This leads us to Figure 2a which is the phase plane for this example.

Now we consider the system with diffusion. We get our initial and boundary conditions from assuming the UK is a large one-dimensional forest, where the  $x$ -axis represents the current position in the forest and when the forest ends there are no more squirrels. This implies we have Dirichlet boundary conditions. Since the UK was populated with red squirrels and a small group of grey squirrels were introduced then this gives us the initial condition shown in Figure 2b at Time = 0. It can be seen in this simulation that the grey squirrel population dominates the red squirrel population in their local area and then the grey squirrel population spreads.

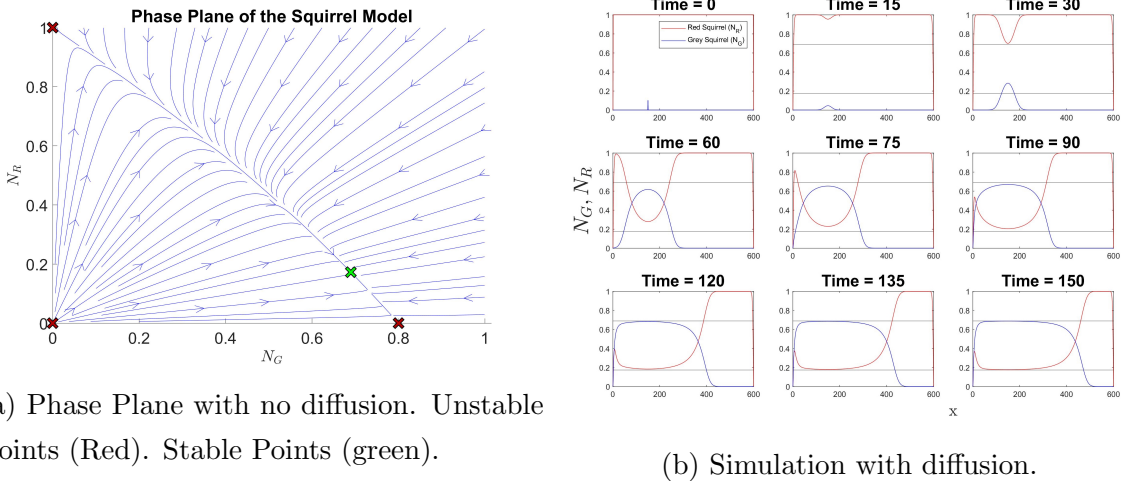


Figure 2: Numerical simulation of PDE (2) with  $D_G = 8$ ,  $D_R = 4$ ,  $K_R = 1$ ,  $K_G = 0.8$ ,  $r_G = r_R = 1$ ,  $\alpha_R = 1.2$  and  $\alpha_G = 0.8$ .

Additionally, we can see that the analysis of the non-diffusion case gives us the values the squirrel population density will converge to. These are denoted by two horizontal lines on each graph in Figure 2b.

This is because diffusion in a reaction-diffusion equation causes instability.

### 3.3 Simulation of Red Squirrel Extinction in 2D

We will solve the PDE system (2) in two spatial dimensions. We will use variables  $D_G = 0.5$ ,  $D_R = 0.5$ ,  $K_G = K_R = 1$ ,  $r_G = r_R = 1$ ,  $\alpha_R = 1.4$  and  $\alpha_G = 0.6$ . Then we get our non-dimensional constants from (4) being

$$r = 1, \beta_G = 0.6, \beta_R = 1.4, D = 1. \quad (10)$$

By analysing the case with no diffusion, there is no coexistence state in the positive quadrant ( $N_G, N_R > 0$ ). We have  $\beta_G < 1$  which implies the red squirrel dominance fixed point is unstable. Also, we have  $\beta_R > 1$  which implies the grey squirrel dominance fixed point is stable. We use the same reasoning for the initial and boundary conditions we used in the previous example. Therefore, we predict that a small group of grey squirrels will spread and dominate the system. This corresponds with our numerical simulation which is shown in Figure 3.

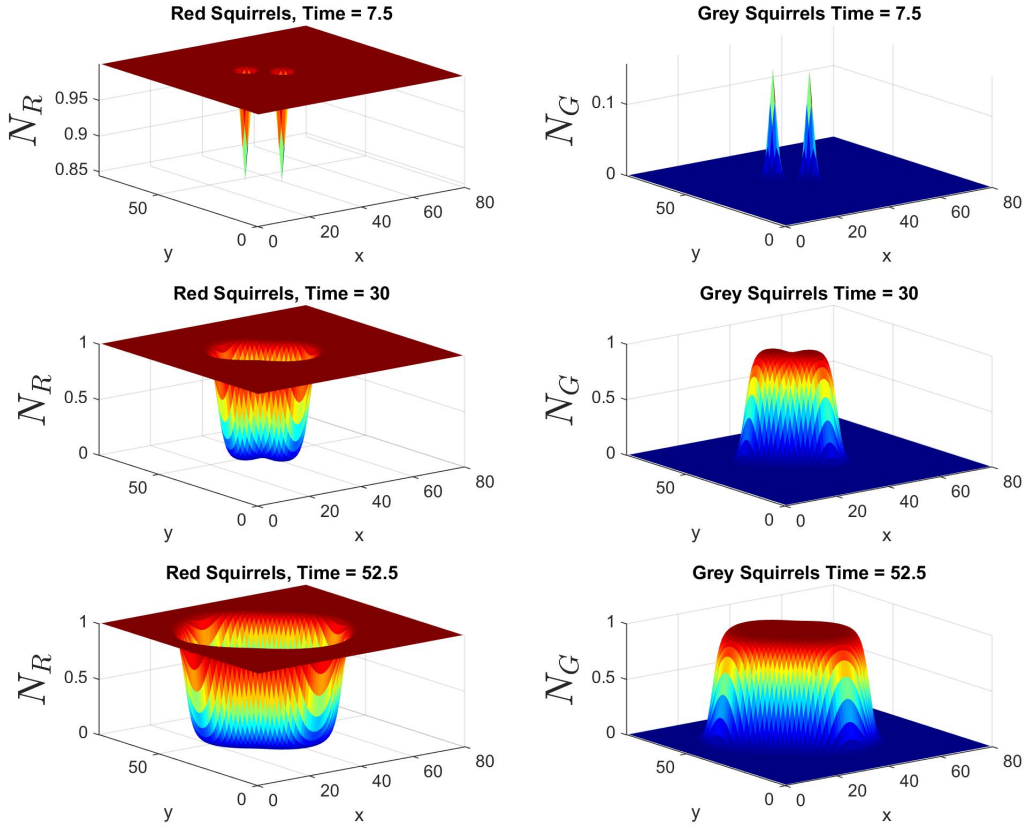


Figure 3: Numerical simulation of the PDE (2) in 2 spatial dimensions with  $D_G = 0.5$ ,  $D_R = 0.5$ ,  $K_G = K_R = 1$ ,  $r_G = r_R = 1$ ,  $\alpha_R = 1.4$  &  $\alpha_G = 0.6$ .

Additionally, the graph in Figure 3 replicates the numerical results that were calculated in [3].

## 4 Gatenby and Gawlinski with Wound Healing

This model describes the invasion of cancer cells and the destruction of normal tissue in the vicinity. We can compare this to the previous model (2) by replacing the red squirrel population density with healthy tissue density and replacing the grey squirrel population density with cancer tissue density.

Additionally, we will consider the Warburg effect this is a phenomenon where cancer cells prefer to utilise anaerobic glycolysis rather than aerobic glycolysis even under normal oxygen levels also known as normoxia. This causes an excess concentration of  $H^+$  ions. The lactic acid ( $H^+$  ions) diffuses into the neighbouring tissue causing

death of healthy tissue, this process works because normal cells have an optimal pH of 7.4 but cancer cells have an optimal pH of 6.8. This leads us to the PDE stated in [1] which is

$$\begin{cases} \partial_t N_1 = r_1 N_1 \left(1 - \frac{N_1}{K_1} - \alpha_2 \frac{N_2}{K_2}\right) \boxed{-d_1 L N_1}, \\ \partial_t N_2 = r_2 N_2 \left(1 - \frac{N_2}{K_2} - \alpha_1 \frac{N_1}{K_1}\right) \boxed{-d_2 L N_2} \boxed{+ \nabla \cdot \left(D_2 \left(1 - \frac{N_1}{K_1}\right) \nabla N_2\right)}, \\ \partial_t L = r_3 N_2 - d_3 L + D_3 \nabla^2 L. \end{cases} \quad (11)$$

Where  $\cdot_1, \cdot_2$  represent healthy and cancer cells respectively. Also, we have a non-linear diffusion term in equation (11) for the cancer cells shown boxed in blue. This models cancer cells only being able to spread in the absence of healthy cells. But the tumour can still spread because lactic acid kills healthy cells. Also, the Warburg Effect terms are boxed in orange. From our numerical simulations for the PDE system (11) shown in Figure 4b, we see that a gap is formed. Healthy cells view the gap caused by lactic acid as a wound and will attempt to heal the wound, this can be modelled by the equation

$$\begin{cases} \partial_t N_1 = r_1 N_1 \left(1 - \frac{N_1}{K_1} - \alpha_2 \frac{N_2}{K_2}\right) - d_1 L N_1 \boxed{+ \nabla \cdot \left(D_1 \left(1 - \frac{N_2}{K_2}\right) \nabla N_1\right)}, \\ \partial_t N_2 = r_2 N_2 \left(1 - \frac{N_2}{K_2} - \alpha_1 \frac{N_1}{K_1}\right) - d_2 L N_2 + \nabla \cdot \left(D_2 \left(1 - \frac{N_1}{K_1}\right) \nabla N_2\right), \\ \partial_t L = r_3 N_2 - d_3 L + D_3 \nabla^2 L. \end{cases} \quad (12)$$

As can be seen in the PDE system (12) we have added a nonlinear diffusion term for the healthy cells denoted by the red box. This simulates the healthy cells only diffusing when there is no presence of cancer cells. Gatenby and Gawlinski were criticised for omitting this term.

To further analyse the PDE system (12) we non-dimensionalize using the scaled variables

$$N_1 = u K_1, \quad N_2 = v K_2, \quad L = \frac{r_3 K_2 \ell}{d_3}, \quad t = \frac{\tilde{t}}{r_1}, \quad \vec{x} = \sqrt{\frac{D_3}{r_1}} \tilde{\vec{x}}. \quad (13)$$

We will define the constants

$$\delta_1 = \frac{d_1 r_3 K_2}{r_1 d_3}, \quad \delta_2 = \frac{d_2 r_3 K_2}{r_1 d_3}, \quad \delta_3 = \frac{d_3}{r_1}, \quad (14)$$

$$p_2 = \frac{r_2}{r_1}, \quad \Delta_1 = \frac{D_1}{D_3}, \quad \Delta_2 = \frac{D_2}{D_3}, \quad (15)$$

this leads to the PDE system

$$\begin{cases} \partial_{\tilde{t}} u = u(1 - u - \alpha_2 v) - \delta_1 u \ell + \Delta_1 \tilde{\nabla} \cdot ((1 - v) \tilde{\nabla} u), \\ \partial_{\tilde{t}} v = p_2 v(1 - v - \alpha_1 u) - \delta_2 v \ell + \Delta_2 \tilde{\nabla} \cdot ((1 - u) \tilde{\nabla} v), \\ \partial_{\tilde{t}} \ell = \delta_3(v - \ell) + \tilde{\nabla} \cdot \tilde{\nabla} \ell. \end{cases} \quad (16)$$

We discuss how to numerically simulate the PDE system (16) in Appendix A.

## 4.1 ODE Analysis

We now remove diffusion to get the system of ODE's

$$\frac{du}{d\tilde{t}} = u(1 - u - \alpha_2 v) - \delta_1 u \ell \quad (17)$$

$$\frac{dv}{d\tilde{t}} = p_2 v(1 - v - \alpha_1 u) - \delta_2 v \ell, \quad (18)$$

$$\frac{d\ell}{d\tilde{t}} = \delta_3(v - \ell). \quad (19)$$

We do this to analyse the fronts once the wave has passed. This gives the linearised system

$$\begin{bmatrix} 1 - 2u - \alpha_2 v - \delta_1 \ell & -\alpha_2 u & -\delta_1 u \\ -\alpha_1 p_2 u & p_2(1 - 2v - \alpha_1 u) - \delta_2 \ell & -\delta_2 v \\ 0 & \delta_3 & -\delta_3 \end{bmatrix}. \quad (20)$$

Then by doing standard analysis we calculate the fixed points and their stability

**Extinction, Trivial Solution,  $v = u = \ell = 0$ .** This leads to the Jacobian matrix (20) having eigenvalues  $\lambda = 1, \lambda = p_2$  and  $\lambda = -\delta_3$ . Since some of these eigenvalues are positive the fixed point is unstable.

**Healthy,  $u = 1, v = \ell = 0$ .** This leads to the Jacobian matrix (20) having eigenvalues  $\lambda = -1, \lambda = -\delta_3$  and  $\lambda = -p_2(\alpha_1 - 1)$ . The point is unstable when  $\alpha_1 < 1$  and stable when  $\alpha_1 > 1$ .

**Tumour,  $u = 0, v = \ell = \frac{p_2}{p_2 + \delta_2}$ .** This leads to the Jacobian matrix (20)

$$\frac{1}{\delta_2 + p_2} \begin{bmatrix} p_2(1 - \alpha_2 - \delta_1) + \delta_2 & 0 & 0 \\ -\alpha_1 p_2^2 & -p_2^2 & -\delta_2 p_2 \\ 0 & \delta_3(\delta_2 + p_2) & -\delta_3(\delta_2 + p_2) \end{bmatrix} \quad (21)$$

which has eigenvalues

$$\lambda = 1 - \frac{p_2(\alpha_2 + \delta_1)}{\delta_2 + p_2}, \quad (22)$$

$$\lambda_{\pm} = \frac{-(\delta_2 \delta_3 + \delta_3 p_2 + p_2^2) \pm \sqrt{(\delta_2 \delta_3 + \delta_3 p_2 + p_2^2)^2 - 4\delta_3 p_2(\delta_2^2 + 2\delta_2 p_2 + p_2^2)}}{2(\delta_2 + p_2)}. \quad (23)$$

We have  $\lambda_{\pm} < 0$  since  $(\delta_2\delta_3 + \delta_3p_2 + p_2^2) > \sqrt{(\delta_2\delta_3 + \delta_3p_2 + p_2^2)^2 - 4\delta_3p_2(\delta_2^2 + 2\delta_2p_2 + p_2^2)}$ , if square root is imaginary we take the real part of  $\lambda_{\pm}$  which is negative. Thus for this fixed point to be stable we must have  $\delta_2 + p_2 < p_2(\alpha_2 + \delta_1)$ . And the fixed point is unstable when  $\delta_2 + p_2 > p_2(\alpha_2 + \delta_1)$ .

**Coexistence,** This state is located at  $v = \ell$  with  $u$  and  $v$  satisfying

$$\begin{bmatrix} 1 & \alpha_2 + \delta_1 \\ \alpha_1 & 1 + \frac{\delta_2}{p_2} \end{bmatrix} \begin{bmatrix} u \\ v \end{bmatrix} = \begin{bmatrix} 1 \\ 1 \end{bmatrix}. \quad (24)$$

We consider the case when  $1 + \frac{\delta_2}{p_2} - \alpha_1(\alpha_2 + \delta_1) \neq 0$ . This gives us

$$u = \frac{1 + \frac{\delta_2}{p_2} - \alpha_2 - \delta_1}{1 + \frac{\delta_2}{p_2} - \alpha_1(\alpha_2 + \delta_1)}, \quad v = \frac{1 - \alpha_1}{1 + \frac{\delta_2}{p_2} - \alpha_1(\alpha_2 + \delta_1)}. \quad (25)$$

We now want to find when the coexistence fixed point is stable. We want the healthy fixed point to be unstable this implies  $1 - \alpha_1 > 0$  and we want the tumour fixed point to be unstable this implies  $1 + \frac{\delta_2}{p_2} - \alpha_2 - \delta_1 > 0$ . For the point (25) to be in the valid domain  $(u, v, \ell > 0)$  we must have  $1 + \frac{\delta_2}{p_2} - \alpha_1(\alpha_2 + \delta_1) > 0$ . To help us calculate the stability of this point we introduce notation

$$\kappa = p_2(1 - \alpha_1(\alpha_2 + \delta_1)) + \delta_2 > 0, \quad (26)$$

$$\xi = p_2(1 - \delta_1 - \alpha_2) + \delta_2 > 0, \quad (27)$$

$$\eta = p_2(1 - \alpha_1) > 0. \quad (28)$$

We note with this notation  $u = \frac{\xi}{\kappa}, v = \frac{\eta}{\kappa}$ . Now we substitute this into the Jacobian (20) to get

$$J = \frac{1}{\kappa} \begin{bmatrix} -\xi & -\alpha_2\xi & -\delta_1\xi \\ -\alpha_1p_2\eta & -p_2\eta & -\delta_2\eta \\ 0 & \delta_3\kappa & -\delta_3\kappa \end{bmatrix} \quad (29)$$

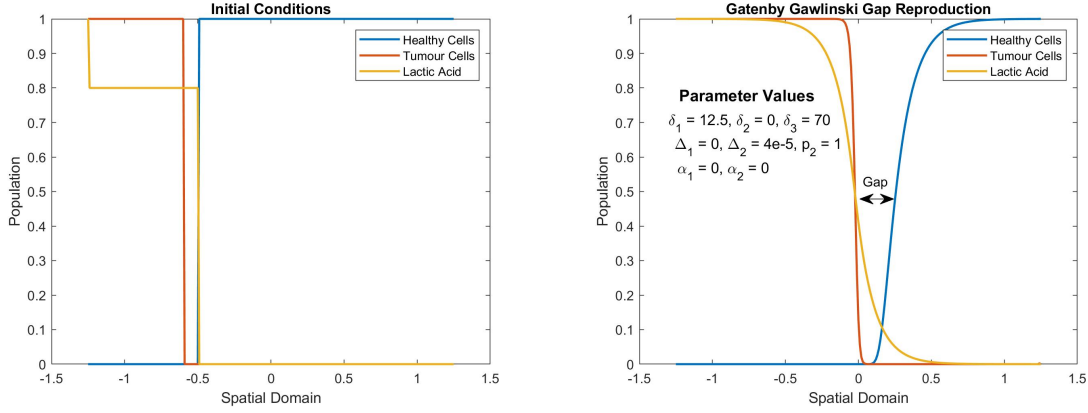
We calculate the signs of the  $\lambda$ 's satisfying  $\det(J - \lambda I) = 0$ . This leads to the equation

$$-\lambda^3 - \frac{\lambda^2}{\kappa}(\delta_3\kappa + \eta p_2 + \xi) - \frac{\lambda}{\kappa^2}[(1 - \alpha_1\alpha_2)\eta\xi p_2 + \delta_3\kappa(\eta(p_2 + \delta_2) + \xi)] - \frac{\delta_3\eta\xi}{\kappa} = 0 \quad (30)$$

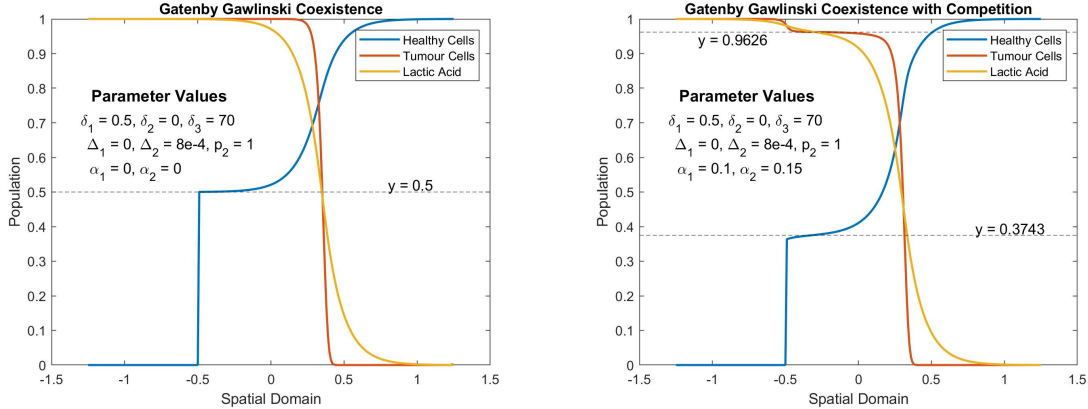
We can use Descartes Rule of Signs which is described at [4]. If we have zero sign changes therefore we have 0 positive real roots for  $\lambda$ . Additionally, we have 3 or 1 negative real roots. When the  $\lambda$  is imaginary then the point is stable but not asymptotically stable. This means to be stable we must have  $\alpha_1\alpha_2 - 1 < \delta_3\kappa \frac{\eta(p_2 + \delta_2) + \xi}{\eta\xi p_2}, \kappa > 0, \xi > 0$  and  $\eta > 0$ . This can be simplified to,  $\alpha_1\alpha_2 - 1 < 0, \kappa > 0, \xi > 0$  and  $\eta > 0 \implies$  stability.

## 4.2 Simulations of G & G without Wound Healing

Where the numerical simulations denoted in Figures 4b, 4c and 4d have initial conditions shown in Figure 4a and simulates the non-dimensional Gatenby and Gawlinski with wound healing system (16) at time  $t = 46.2$ .



(a) Initial conditions for all G and G based numerical simulation ( $t = 0$ ). (b) Tumour dominance with no competition, shows gap is formed.



(c) Coexistence state with no competition. (d) Coexistence state with competition.

Figure 4: Numerical Simulation of Chemo and Bicarbonate Therapy

In Figure 4b we have a numerical simulation which shows a gap forming. This is bad as the tumour cells can spread into the gap.

In Figure 4c for our numerical simulation we have parameters  $\xi = 0.5, \eta = 1$  and  $\kappa = 1$ . Since  $\alpha_1\alpha_2 = 0 < 1$  this implies  $u = \frac{\xi}{\kappa} = 0.5, v = \ell = \frac{\eta}{\kappa} = 1$  is a stable fixed point. It can be seen in Figure 4c once the wavefront has passed the system converges to these values denoted in dashed lines.

In Figure 4d for our numerical simulation we have parameters  $\xi = 0.35, \eta = 0.9$

and  $\kappa = 0.935$ . Since  $\alpha_1\alpha_2 = 0.015 < 1$  this implies  $u = \frac{\xi}{\kappa} \approx 0.3743, v = \ell = \frac{\eta}{\kappa} \approx 0.9626$  is a stable fixed point. It can be seen in Figure 4d once the wavefront has passed the system converges to these values denoted in dashed lines.

It can be seen that for numerical simulations in Figure 4c and Figure 4d that  $u, v$  and  $\ell$  do not converge to the dashed lines for  $x < -0.5$  this is because the initial condition shown in Figure 4a has the healthy cells equal to zero ( $u = 0$ ) and since there is no wound healing this means there is no diffusion for the healthy cells thus since  $u = 0, v = \ell = 1$  is an unstable fixed point it remains the same as its initial condition.

However, there is still diffusion with respect to the cancer cells, this can be seen since  $v \neq 1$  on the entire domain  $x < -0.5$ . This is explained by looking at the ODE (17), when  $u = 0$  this implies  $\dot{v} = 0$  therefore  $v$  must remain zero. Therefore, in this simulation for  $u = 0$  we have  $\dot{v} = p_2v(1 - v)$  this means for this ODE  $v = 1$  is stable and we have the  $\dot{v}$  changing  $v$  so it approaches  $v$ . Thus in the domain  $x < -0.5$  the system wants to be in the state  $u = 0, v = \ell = 0$ , it may sound like it is stable but that is only the case since  $u$  is forced to be zero.

### 4.3 Simulations of G & G with Wound Healing

The numerical simulation in Figures 5a and 5b have initial condition shown in Figure 4a and simulates the system 16.

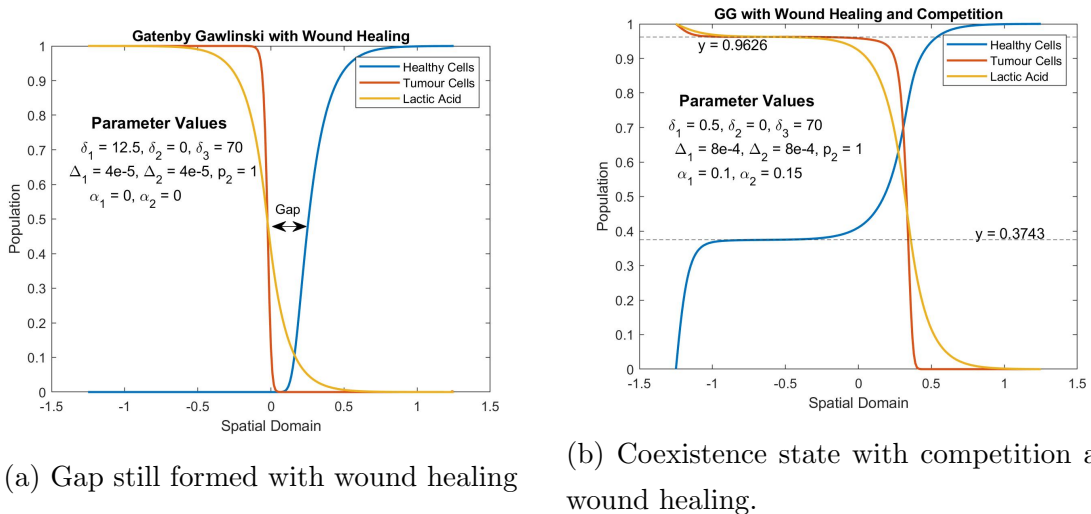


Figure 5: Numerical Simulation of Chemo and Bicarbonate Therapy ( $t = 46.2$ ).

As can be seen by comparing numerical simulations from Figure 5a and Figure 4b

we can see adding wound healing is not enough to prevent gap formation.

Now we compare numerical simulations from Figure 5b and Figure 4d. We notice the main difference is the domain  $x < -0.5$  this is because there is wound healing and this displaces  $u$  from  $u = 0$ . Thus, the system converges to our expected results denoted by the dashed line.

## 5 Treatments

We would like to find a treatment that prevents gap formation because this will make it more difficult for the tumour to spread. Also, we are interested in any treatment that can slow down the invading wave front. We now introduce a modified version of the non-dimensional Gatenby and Gawlinski system with wound healing (16) which is

$$\begin{cases} \partial_t u = \boxed{\beta_1} u (1 - u - \alpha_2 v) - \delta_1 \ell u + \Delta_1 \nabla \cdot ((1 - v) \nabla u), \\ \partial_t v = \boxed{\beta_2} p_2 v (1 - v - \alpha_1 u) - \delta_2 \ell v + \Delta_2 \nabla \cdot ((1 - u) \nabla v) \boxed{-\gamma v \delta(t - T)}, \\ \partial_t \ell = \delta_3 (v - \ell) + \nabla \cdot \nabla \ell \boxed{-p_3 \ell}, \end{cases} \quad (31)$$

where each different coloured box corresponds to a different treatment which we discuss in the next few sub-sections. Also,  $\delta(\cdot)$  denotes the Dirac delta function. We used a finite difference method for the numerical simulation of (31), the code and boundary conditions are discussed in Appendix A.

### 5.1 Chemotherapy

Chemotherapy targets cells which divide themselves at a faster rate this is done by inhibiting mitosis (cell division) [5]. Therefore, tumour cells are targeted. However, chemotherapy also kills some of the healthy cells. We model the chemotherapy by multiplying the reproduction rates  $r_{1,2}$  of (12) by  $\beta_{1,2} \in (0, 1)$ . This leads to the addition of the boxed terms coloured in orange for the non-dimensional equation (31).

### 5.2 Bicarbonate Therapy

By adding bicarbonate to the system the tumour pH is increased which inhibits the growth of tumour cells [6]. This treatment is done by consuming alkaline water. We have  $p_3$  represents the dimensionless constant controlling the rate at which the

bicarbonate neutralises the lactic acid. Thus, we have the boxed term coloured in blue added to the non-dimensional model (31).

### 5.3 Surgery

By applying surgery we cut out the cancer cells [7] at a certain time  $T > 0$  with effectiveness  $\gamma \in [0, 1]$ . We assume that the surgery does not damage the healthy cells. This gives us the boxed term coloured in red for the non-dimensional PDE system (31).

### 5.4 Numerical Simulations of Individual Treatments

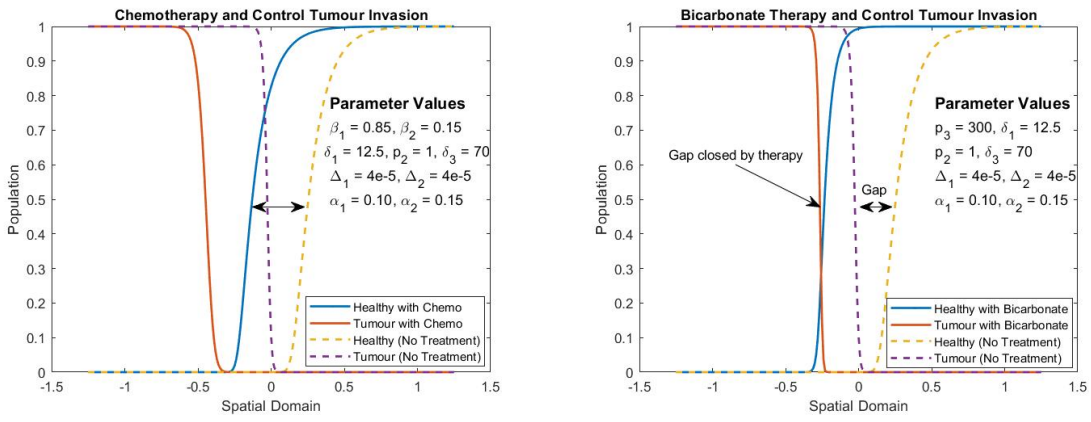


Figure 6: Numerical Simulation of Chemo and Bicarbonate Therapy ( $t = 46$ ).

In Figure 6a we have the numerical simulation of applying chemotherapy to cancer cells. The solid lines represent the numerical simulation with the treatment and the dashed lines represent the numerical simulation without treatment thus  $\beta_1 = \beta_2 = 1$ . It can be seen chemotherapy reduces the wave speed leading to the tumour taking longer to spread.

In Figure 6b we have the numerical simulation of applying bicarbonate therapy to cancer cells. The solid lines represent the numerical simulation with the treatment and the dashed lines represent the numerical simulation without treatment thus  $p_3 = 0$ . Thus from the simulation bicarbonate therapy reduces lactic acid which allows for the healthy cells to spread into the gap. Thus bicarbonate therapy removes the gap making it harder for the tumour to spread and reducing the invading wave speed.

The numerical simulations shown in Figures 6a and 6b have the initial condition shown in Figure 4a. The initial condition states the tumour is located in the domain  $x \leq -0.6$ . Since in both simulations for chemo and bicarbonate therapy we can see the tumour has spread past  $x = 0.6$ , this implies the therapy is not enough to stop the tumour only slow it down.

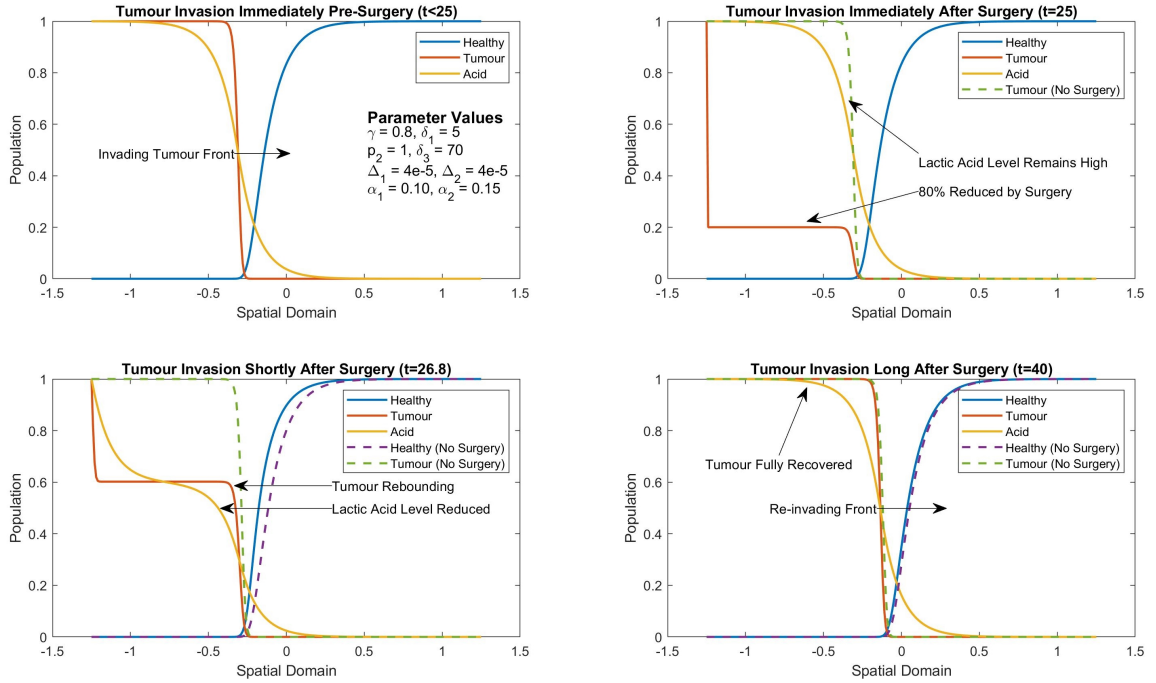


Figure 7: Numerical simulation of surgery performed on invading tumour,  $0 < t < 50$ , 80% tumour removal, i.e.  $\gamma = 0.8$ , at  $T = 25$ .

Figure 7 shows the numerical simulation of using surgery as a treatment with the initial condition shown in Figure 4a. We denote the dashed lines as the numerical simulation without surgery. It is clear by looking at the results at  $t = 40$  that there is a negligible difference between the position of the invading tumour with surgery and the invading tumour without surgery. Therefore, surgery does not provide any long term benefit to stopping the tumour spread. However, when the effectiveness of the surgery is 100% (i.e.  $\gamma = 1$ ) then the tumour is removed but anything less than perfect will cause the tumour to grow back.

## 5.5 Numerical Simulations of Combined Treatments

In Figure 8 we have a numerical simulation which uses bicarbonate and chemotherapy on initial conditions shown in Figure 4a.

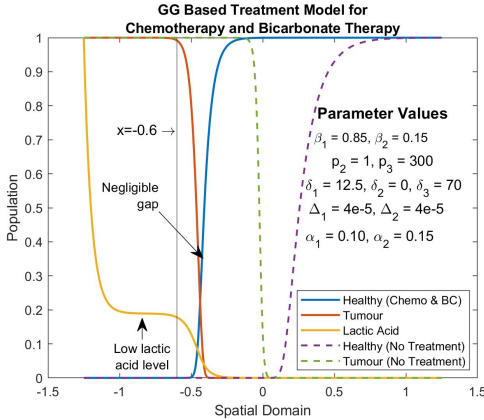


Figure 8: Numerical simulation of bicarbonate and chemo therapy performed on invading tumour ( $t = 46.2$ ).

The vertical line at  $x = -0.6$  denotes the position where the tumour front starts, it shows that by using bicarbonate therapy the gap size is reduced and by using chemotherapy the invading wavefront speed is significantly reduced. This leads to a wavefront which is considerably closer to the initial position of the tumour front compared to doing the treatments independently which is shown in Figures 6b and 6a. However, this only slows the tumour front, given time the cancer cells will dominate the system.

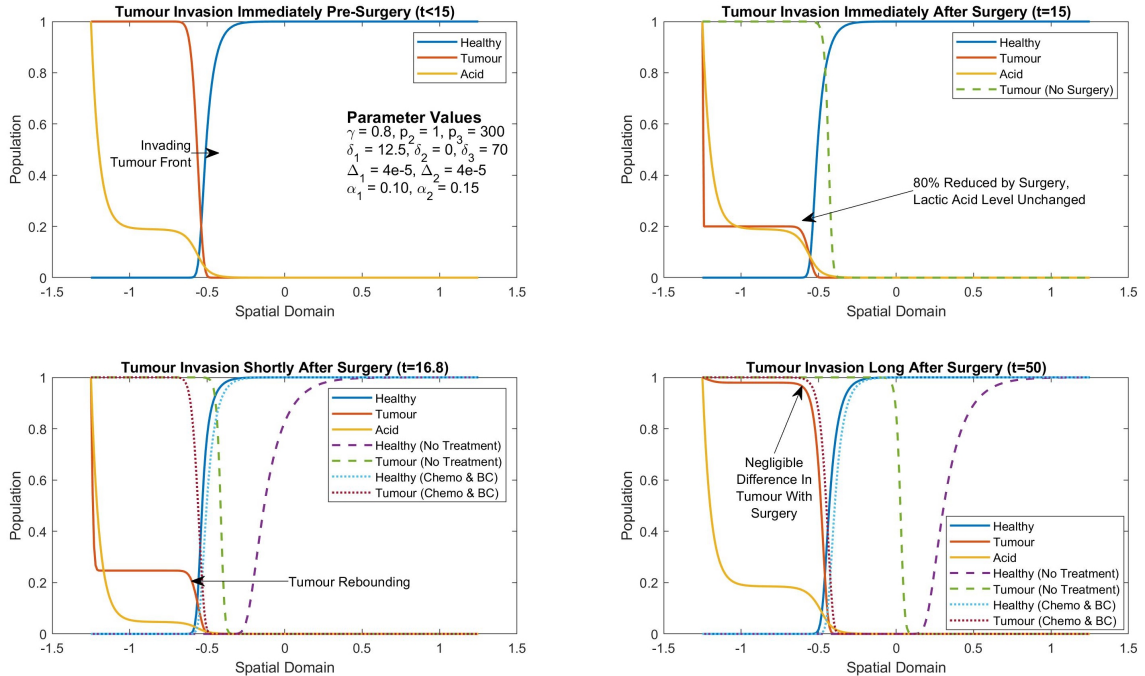


Figure 9: Numerical simulation of bicarbonate therapy, chemo therapy and surgery performed on invading tumour, with 80% tumour removal, i.e.  $\gamma = 0.8$ , at  $T = 15$ . Also,  $\beta_1 = 0.85$  and  $\beta_2 = 0.15$

In Figure 9 we have a numerical simulation that involves surgery, chemotherapy and bicarbonate therapy denoted by solid lines. Also, the dashed lines denote a

numerical simulation without treatment and the dotted lines represent a simulation with bicarbonate and chemotherapy. By looking at  $t = 50$  it is clear to see that a long time after surgery the difference between having surgery with chemo and bicarbonate therapy compared to having only chemo and bicarbonate therapy is negligible. This strongly indicates along with Figure 7 surgery is not a viable option for stopping a tumour.

## 6 Conclusion

We have investigated the Fisher equation and the squirrel model numerically and analytically by calculating the convergence of the system once the wavefront has passed. These results coincide giving us a strong indication our numerical and convergence results are correct. Furthermore, by including the Warburg effect we investigated the Gatenby and Gawlinski model and proved numerical results stated in their paper including the formation of a gap given certain parameters. Also, we added wound healing and noticed the gap still formed thus the criticisms of their paper for excluding wound healing are unfounded.

For our treatments, we find combining bicarbonate therapy and chemotherapy leads to good results and decreases the wave speed of the invading tumour the most. Also, bicarbonate therapy is very effective at reducing gap size but for this treatment to work large amounts of alkaline needs to be inserted into the tissue, this could lead to other side effects like alkaline poisoning. Additionally, we found in the long term surgery is not a viable treatment and is only effective if all the cancer cells are removed.

In this project, my individual extensions were doing more work on stability analysis this included finding parameter restrictions for stable coexistence states to exist in the Gatenby and Gawlinski model with wound healing. Also, changing and implementing new numerical simulations to show that when the wavefront had passed, the numeric solution converged to the stable state. Furthermore, it included looking at the combination of treatments. Finally, it included a better comparison between treatments with and without surgery.

Further research and development would be focused on implementing more realistic models one example would be to include multiple tumour cell types which are described in [8] and multiple healthy cell types like fibroblast for wound healing and epithelium. Also, adding more treatments and comparing different treatment parameters for the greatest reduction in wavefront speed.

## References

- [1] Robert A. Gatenby and Edward T. Gawlinski. “A Reaction-Diffusion Model of Cancer Invasion”. In: *Cancer Research* 56.24 (1996), pp. 5745–5753. ISSN: 0008-5472. eprint: <https://cancerres.aacrjournals.org/content/56/24/5745.full.pdf>. URL: <https://cancerres.aacrjournals.org/content/56/24/5745>.
- [2] Ruth E Baker. “Further Mathematical Biology Lecture Notes”. In: (5.10.2021).
- [3] Akira Okubo et al. “On the spatial spread of the grey squirrel in Britain”. In: *Proceedings of the Royal Society of London. B. Biological Sciences* 238.1291 (1989), pp. 113–125. DOI: 10.1098/rspb.1989.0070. eprint: <https://royalsocietypublishing.org/doi/pdf/10.1098/rspb.1989.0070>. URL: <https://royalsocietypublishing.org/doi/abs/10.1098/rspb.1989.0070>.
- [4] Brilliant. *Descartes’ Rule of Signs*. Last accessed 01.05.2022. 8.01.2019. URL: <https://brilliant.org/wiki/descartes-rule-of-signs/>.
- [5] Mayo Clinic. *Chemotherapy*. Last accessed 06.05.2022. 4.06.2020. URL: <https://www.mayoclinic.org/tests-procedures/chemotherapy/about/pac-20385033>.
- [6] Ian Forrest Robey et al. “Bicarbonate increases tumor pH and inhibits spontaneous metastases.” In: *Cancer research* 69 6 (2009), pp. 2260–8.
- [7] Mayo Clinic. *Cancer treatment*. Last accessed 01.02.2022. 4.06.2020. URL: <https://www.mayoclinic.org/tests-procedures/cancer-treatment/about/pac-20393344>.
- [8] Maximilian A. R. Strobl et al. “Mix & Match: Phenotypic coexistence as a key facilitator of solid tumour invasion”. In: *bioRxiv* (2019). DOI: 10.1101/750810. eprint: <https://www.biorxiv.org/content/early/2019/08/30/750810.full.pdf>. URL: <https://www.biorxiv.org/content/early/2019/08/30/750810>.

## A Code For Numerical Simulation

As a group, we used the finite difference method to numerically calculate solutions to the systems of partial differential equations stated in this paper. We used the code from 'NonDSpread\_WH.BC\_Chemo\_Surgery.m' to solve the PDE (31). And we

used boundary conditions  $N_1(x = -1.25, t) = N_2(x = 1.25, t) = L(x = -1.25, t) = 1$ ,  $N_1(x = 1.25, t) = N_2(x = -1.25, t) = L(x = 1.25, t) = 0$ .

```

1 function [N_1,N_2,L] = NonDSpread_WH_BC_Chemo_Surgery(d_1,p_2,p_3,
2 D_1,D_2,d_3,a_1,a_2,b_1,b_2,S,T)
3 %
4 % This function simulates the non-dimensional Gatenby Gawlinski
5 % Model with
6 % wound healing, bicarbonate therapy, chemotherapy and surgery.
7 %
8 % INPUTS: (All non dimensional constants)
9 %         d_1 - Constant controlling death rate of healthy due to
10 %               lactic acid
11 %         p_2 - Ratio of reproduction of tumour and healthy cells
12 %         p_3 - Ratio of bicarbonate rate to healthy cell production
13 %         D_1 - Ratio of wound healing to acid diffusion constants
14 %         D_2 - Ratio of tumor to acid diffusion constants
15 %         d_3 - Ratio of removal of lactic acid and reproduction of
16 %               healthy
17 %               cells
18 %         a_1 - Competition constant 1
19 %         a_2 - Competition constant 2
20 %         b_1 - Chemo constant for healthy cells
21 %         b_2 - Chemo constant for tumor cells
22 %         S - surgery success constant
23 %         T - Time of surgeries
24 %
25 %
26 % OUTPUTS: (Non Dimensional)
27 %         N_1 - Population of healthy cells over xdom at each timestep
28 %         N_2 - Population of tumor cells over xdom at each timestep
29 %         L - Population of lactic acid over xdom at each timestep
30 %
31 %
32 %
33 %
34 tf = 50;
35 dt = 0.4e-4;
36 dx = 0.01;
37 xdom = -1.25:dx:1.25;
```

```

38 tdom = 0:dt:tf;
39
40 N_1 = zeros(length(xdom),length(tdom));
41 N_2 = zeros(size(N_1));
42 L = zeros(size(N_1));
43
44 % I.C.
45 N_1(:,1) = (xdom>-0.5);
46 N_2(:,1) = (xdom<=-0.6);
47 L(:,1) = 0.8*(xdom<=-0.5);
48
49 % B.C.
50 N_1(1,:) = 1e-15;
51 N_2(1,:) = 1;
52 N_1(end,:) = 1;
53 N_2(end,:) = 1e-15;
54 L(1,:) = 1;
55 L(end,:) = 1e-15;
56
57 %Times of Surgery
58 T = round(T/dt);
59 My_Member = ismember(1:(length(tdom)-1),T);
60
61 for m = 1:(length(tdom)-1)
62     for i = 2:(length(xdom)-1)
63         DN_1 = (1/(2*dx))*(N_1(i+1,m) - N_1(i-1,m));
64         DN_2 = (1/(2*dx))*(N_2(i+1,m) - N_2(i-1,m));
65         DDN_1 = (1/(dx^2))*(N_1(i+1,m) - 2*N_1(i,m) + N_1(i-1,m));
66         DDN_2 = (1/(dx^2))*(N_2(i+1,m) - 2*N_2(i,m) + N_2(i-1,m));
67         DDL = (1/(dx^2))*(L(i+1,m) - 2*L(i,m) + L(i-1,m));
68
69         N_1(i,m+1) = N_1(i,m) + dt*(b_1*N_1(i,m).*(1-N_1(i,m))-a_2*
70             N_2(i,m))-d_1.*L(i,m).*N_1(i,m)+...
71             D_1*(DDN_1));
72
73         N_2(i,m+1) = N_2(i,m) + dt*(b_2*p_2*N_2(i,m)*(1 - N_2(i,m)-
74             a_1*N_1(i,m)) + ...
75             D_2*((1 - N_1(i,m))*DDN_2 - DN_1.*DN_2)) - s*N_2(i,m)*My_Member(m);
76
77         L(i,m+1) = L(i,m) + dt*(d_3*(N_2(i,m) - L(i,m)) + DDL-p_3*L(
78             i,m));
79     end

```

77 **end**  
78 **end**